Mechanisms and Electron Transfer of Prokaryotic Nitrate Reductases

Yiming Luo
Hwa Chong International School, Singapore, 269783, Singapore

Keywords: Prokaryotic Nitrate Reductases, Metalloenzyme, Special Cofactors, Electron Transfer.

Abstract: There are three types of prokaryotic nitrate reductases which are essential in the biological nitrogen cycle, respectively membrane-bound respiratory nitrate reductase (Nar), periplasmic nitrate reductase (Nap) and prokaryotic assimilatory nitrate reductase (Nas). This work summarizes the structures of these three types of nitrate reductases, as well as their nitrate reduction mechanism and electron transfer pathways. They each contain a molybdenum bis-molybdopterin guanine dinucleotide cofactor (Mo-bis-MGD) as the active site for nitrate binding, and they use different numbers and types of iron–sulfur clusters to aid the electron transfer. Nar and Nap use hemes and the quinol–quinone Q cycle as the electron source, whereas Nas relies on flavodoxin or NADH. This work also presents some possible aspects for future research, such as the uniqueness of molybdenum, the large potential barriers in the Nap electron transfer pathway, and unsolved crystal structures of some enzyme subunits that have limited understanding.

1 INTRODUCTION

Nitrogen is an element necessary for all lifeforms because it is a building block of many essential biological molecules such as nucleic acids, amino acids, and proteins. It occurs in various oxidation states, such as dinitrogen (N_2, 0) in the atmosphere, ammonium (NH_4^+, −3) in sediments and minerals, nitrate (NO_3^-, +5) as dissolved species in marine environments (Bebout, Fogel, Cartigny, 2013), and organic nitrogen compounds in organisms. Nitrogen can be converted between these forms, referred to as the nitrogen cycle. Nitrate reductases play an essential role in the nitrogen cycle, by catalyzing the reduction of nitrate to nitrite (NO_2^-), which is ready for further reduction:

$$NO_3^- + 2H^+ + 2e^- \rightarrow NO_2^- + H_2O,\ E^{\ominus} = +420\,\text{mV} \quad \text{(Equation 1)}$$

The aim of this report is to provide a brief introduction of the nitrogen cycle and nitrate reduction pathways, summarize and compare the structures of different prokaryotic nitrate reductases and explore the mechanisms of the Mo-bis-MGD active site, as well as the role of each special cofactor in the entire electron transport chain.

2 COMMON METHODS TO DETERMINE NITRATE REDUCTASE STRUCTURE

Nitrate reductases are a category of metalloenzyme with a molybdenum ion at each of their active sites. Common methods to determine the structure of nitrate reductases include X-ray crystallography, specifically multiwavelength anomalous diffraction (MAD), which provided high-resolution electron density maps for the first crystal structure of periplasmic nitrate reductase (Nap) (Dias, 1999). This identified some unique cofactors present in nitrate reductases: a molybdenum bis-molybdopterin guanine dinucleotide cofactor (Mo-bis-MGD), and an iron–sulfur cluster [4Fe–4S] (Figure 1). To understand the coordination and redox activities of the central Mo ion, electron paramagnetic resonance (EPR) spectroscopy and extended X-ray absorption fine structure (EXAFS) spectroscopy were used, which facilitated the investigation of mechanisms of catalysis (Butler, 1999).

Luo, Y.
Mechanisms and Electron Transfer of Prokaryotic Nitrate Reductases.
DOI: 10.5220/0011219400003443
In *Proceedings of the 4th International Conference on Biomedical Engineering and Bioinformatics (ICBEB 2022)*, pages 505-513
ISBN: 978-989-758-595-1

3 THE BIOLOGICAL NITROGEN CYCLE AND NITRATE REDUCTASES

Nitrogen can be converted between different forms through abiotic processes such as the production of nitrogen monoxide (NO) by lightning:

$$N_2 + O_2 \rightarrow 2NO \quad \text{(Equation 2)}$$

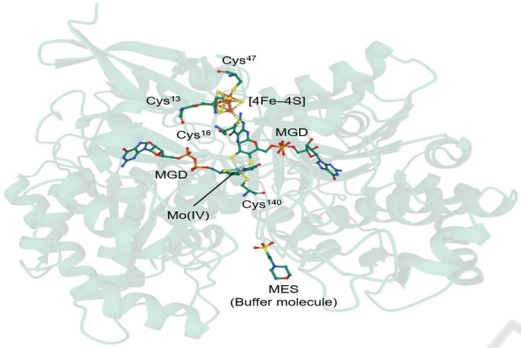

Figure 1: First crystal structure of Nap (subunit NapA) of bacterium *Desulfovibrio desulfuricans* (PDB: 2NAP) obtained by MAD methods. The central Mo (IV) ion is coordinated to two MGDs to form a Mo-bis-MGD cofactor, as well as a cysteine residue Cys^{140}. An iron–sulfur cluster [4Fe–4S] is located nearby for electron transfer.

However, the focus of this report will be the biological nitrogen cycle, where nitrogen is circulated in the biosphere by organisms, predominantly prokaryotes. Different nitrogen compounds are simultaneously oxidized or reduced, and the reductive process can be further divided into two different pathways: nitrate assimilation and denitrification (Cabello, 2009), or dissimilatory nitrate reduction. In nitrate assimilation, NO_3^- are reduced to NH_4^+, a nitrogen source for constructive metabolism, via the only intermediate of NO_2^-, catalyzed by assimilatory nitrate reductase (Nas) and nitrite reductase NirS:

$$NO_3^- \xrightarrow{\text{Nas}} NO_2^- \xrightarrow{\text{NirS}} NH_4^+ \quad \text{(Equation 3)}$$

In contrast to nitrate assimilation, denitrification refers to the catabolic process where NO_3^- acts as the terminal electron acceptor in anaerobic respiration instead of dioxygen (O_2). The terminal products of denitrification can be either nitrous oxide (N_2O) or N_2, via the intermediate stages of NO_2^- and NO. In this case, NO_3^- is reduced to NO_2^- with the catalysis of either Nap or membrane-bound respiratory nitrate reductase (Nar), and the subsequent reduction are catalyzed respectively by nitrite reductases NirS and NirK, NO reductases cNor and qNor, and N_2O reductase (Nos):

$$NO_3^- \xrightarrow{\text{Nar/Nap}} NO_2^- \xrightarrow{\text{NirS/NirK}} NO \xrightarrow{\text{cNor/qNor}} N_2O \xrightarrow{\text{Nos}} N_2 \quad \text{(Equation 4)}$$

This report will only discuss prokaryotic nitrate reductases, i.e. Nas, Nap and Nar, among these enzymes in nitrate reduction processes. A key difference between Nap and Nar is that the active site Mo-bis-MGD of Nap is in the periplasmic space, while Nar's is in the cytoplasm (Moreno-Vivián, 1999). Nar consumes protons to reduce NO_3^- in the cytoplasm and protons are translocated into the periplasm through the oxidation of quinols to quinones ($QH_2 \rightarrow Q + 2H^+ + 2e^-$) in the lipid bilayer by the quinol-oxidizing subunit NarI, thereby enhancing the electrochemical proton gradient to facilitate adenosine triphosphate (ATP) synthesis, while Nap reduces NO_3^- in the periplasm so there is no proton translocation (Kuypers, 2018) (Figure 2).

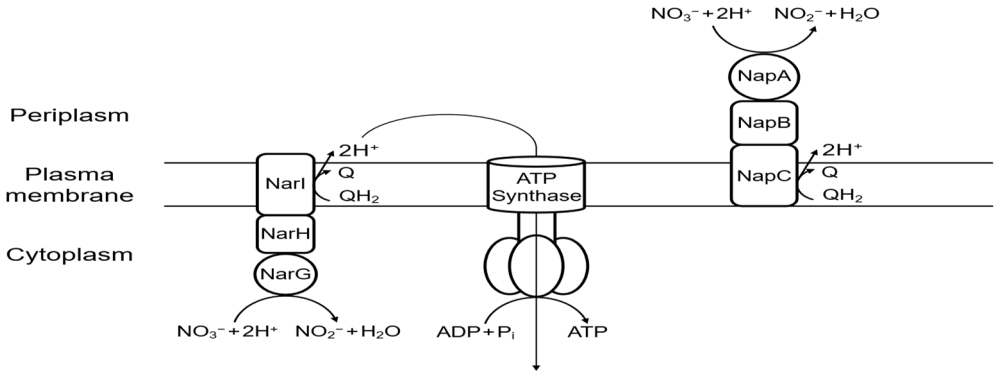

Figure 2: Difference in location and contribution of ATP synthesis between Nar and Nap. The active sites where Mo-bis-MGD is present are represented by circles, i.e. NarG and NapA.

4 SPECIAL COFACTORS PRESENT IN PROKARYOTIC NITRATE REDUCTASES

4.1 Mo-Bis-MGD

Mo-containing enzymes can be categorized into 3 families with similar general structures, all of which contain at least one MGD molecule each (Figure 3), respectively the xanthine oxidase family, the dimethyl sulfoxide (DMSO) reductase family, and the sulfite oxidase family (Moura, 2004) (Figure 4a). Though eukaryotic nitrate reductases (eukNR) belong to the sulfite oxidase family, all prokaryotic nitrate reductases are from the DMSO reductase family, where the central Mo ion is coordinated to two MGD molecules and one or two other ligands (Sparacino-Watkins, 2014) (Figure 4b).

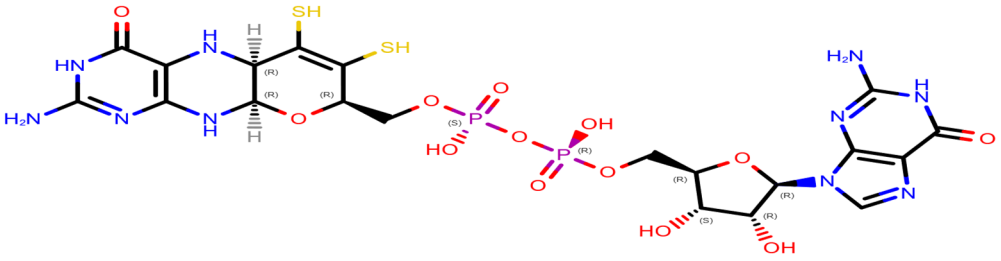

Figure 3: The structure of MGD.

The two sulfhydryl groups (colored yellow in Figure 3) are responsible for Mo-coordination. Although thiols generally have no net charge in neutral pH, sulfhydryl groups are deprotonated and coordinate as thiolates in Mo-bis-MGD (Moura, 2004). This is because highly charged Mo ions can greatly stabilize the conjugate base of thiols, thus lowering the pK_a value of sulfhydryl groups in MGD (Lippard, 1994).

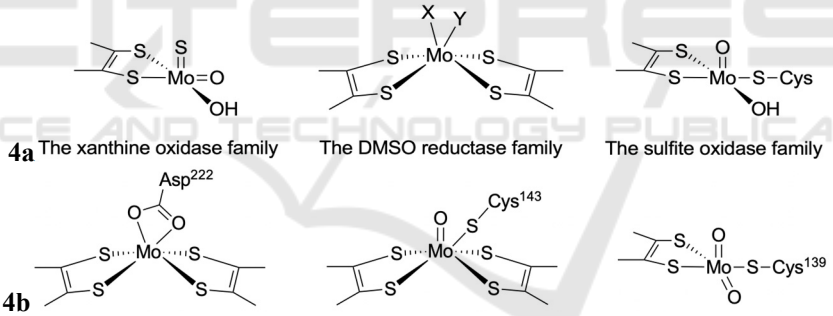

Figure 4: (a) General structures of the three Mo-containing enzyme families. X and Y represent any ligand, either singly or doubly bonded to the Mo ion. The −OH ligands may be replaced by $-OH_2$ or =O. (b) Some examples of Mo active sites. From left to right: NarG (oxidized form) from *Escherichia coli* (PDB: 1Q16), NapA (oxidized form) from *Escherichia coli* (PDB: 2NYA), eukNR from *Pichia angusta* (PDB: 2BII). The first two (Nap, Nar) belong to the DMSO reductase family while the last one (eukNR) belongs to the sulfite oxidase family.

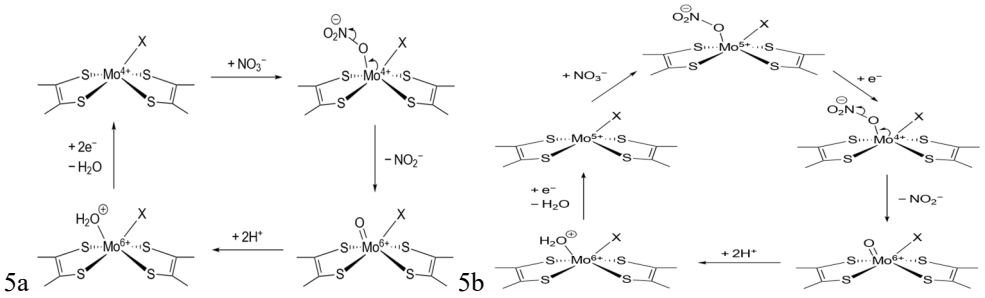

Figure 5: Two different proposed mechanisms of nitrate reduction at the Mo-bis-MGD active site. Though both mechanisms have been proposed, Figure 5b shows the more widely accepted mechanism.

The central Mo ion has variable oxidation states of IV, V and VI. Two different mechanisms of nitrate reduction at the Mo-bis-MGD active site have been proposed (Sparacino-Watkins, 2014) (Figure 5a and 5b). Nitrate reduction starts from the reduced form, where the Mo ion is in the oxidation state of IV or V and is only penta-coordinated with an empty binding site for NO_3^-. Mo(V) ion will then gain an electron, because the binding of NO_3^- raises its redox potential, making it more easily reduced (Richardson, 2007) (Figure 5b). Since nitrogen is reduced from +5 to +3, the coordinated NO_3^- gains two electrons from Mo(IV), oxidizing it to be Mo(VI), with electron configuration [Kr]. The Mo-bis-MGD cofactor is now in its oxidized form, where an oxo ligand is left coordinated to Mo(VI). It is then protonated and leaves as water, reducing Mo(VI) back to either Mo(IV) (Figure 5a) or Mo(V) (Figure 5b) for further reduction of NO_3^-. Regardless of the pathway, two electrons in total are transferred in each cycle.

However, in the crystal structure of *E. coli* NarG (PDB: 1Q16, leftmost in Figure 4b), a bidentate Asp^{222} was discovered, which might block the binding of NO_3^-. Besides, it was concluded that the active site was in its oxidized form, i.e. Mo(VI), but the oxo ligand that appeared in the proposed mechanism was absent. In fact, there are different *E. coli* NarG Mo-bis-MGD structures in the Protein Data Bank (Figure 6).

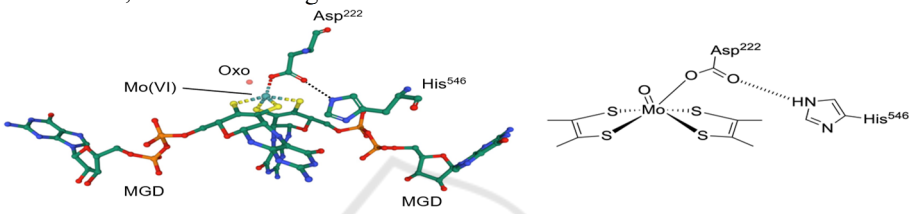

Figure 6: A different structure of the Mo-bis-MGD active site of *E. coli* NarG (PDB: 1R27).

Figure 6 shows another oxidized form of the active site, where the bidentate Asp^{222} is now only singly coordinated to the Mo ion, and the other carboxylate O is hydrogen-bonded to the ε-nitrogen of His^{546}. Although the two structures are different, their amino acid sequences are identical. The difference may be caused by the protonation state of His^{546}, or structural flexibility of the active site. However, further investigation is required to conclude whether both forms are involved in the catalysis of nitrate reduction (Jormakka, 2004).

The proposed mechanisms in Figure 5 also have other limitations: it does not take into account of some Nap structures where there are other ligands coordinated to Mo in addition to a cysteine. At *Rhodobacter sphaeroides* Nap (PDB: 3ML1) Mo-bis-MGD site, a sulfido group (S^{2-}) is doubly bonded to Mo; for *Cupriavidus necator* Nap (PDB: 2JIR), the protein crystal structure shows an additional cyanide ligand coordinated to Mo. They seem to interfere with the binding of NO_3^-, and may also affect the shifting of oxidation state of the Mo ion. A sulfur shift mechanism has been proposed to address the first circumstance (Cerqueira, 2013) (Figure 7). The Mo-bis-MGD site with a sulfido group is described as the inactive state, but when a NO_3^- substrate comes in, the sulfido ligand will undergo structural changes to the active state, where a binding site is vacated and the catalytic reaction can take place as usual.

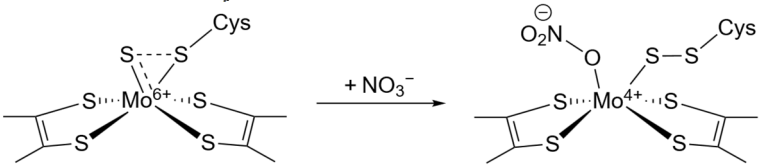

Figure 7: The sulfur shift mechanism.

Tungsten (W) and Mo are from the same group in the periodic table, so they share similar chemical properties, and DMSO reductase (DMSOR) can function with both Mo and W (Stewart, 2000). However, nitrate reductases from the DMSO reductase family, would become inefficient if the Mo ion of Mo-bis-MGD is replaced by W (Sparacino-Watkins, 2014). The reason is still unclear, but one speculation is that W-containing enzymes typically catalyze reactions with lower redox potentials ($E^{\ominus} \leq -420$ mV) (Moura, 2004). Therefore, they may not work for the reduction of NO_3^- whose redox potential is positive (+420 mV).

4.2 Iron–Sulfur Clusters

There are three most common iron–sulfur clusters, respectively [2Fe–2S], [3Fe–4S], and [4Fe–4S] (Broderick, 2004) (Figure 8a). Iron–sulfur clusters are ancient structures developed during evolution. While they are important protein cofactors primarily responsible for electron transfer, they also have other functions such as DNA damage repair (Brzóska, 2006). Iron–sulfur clusters transport electrons through the alteration of Fe oxidation state between +2 and +3, and since each cluster contains more than one Fe ion, it may exhibit multiple overall oxidation states (Beinert, 2000) (Figure 8b).

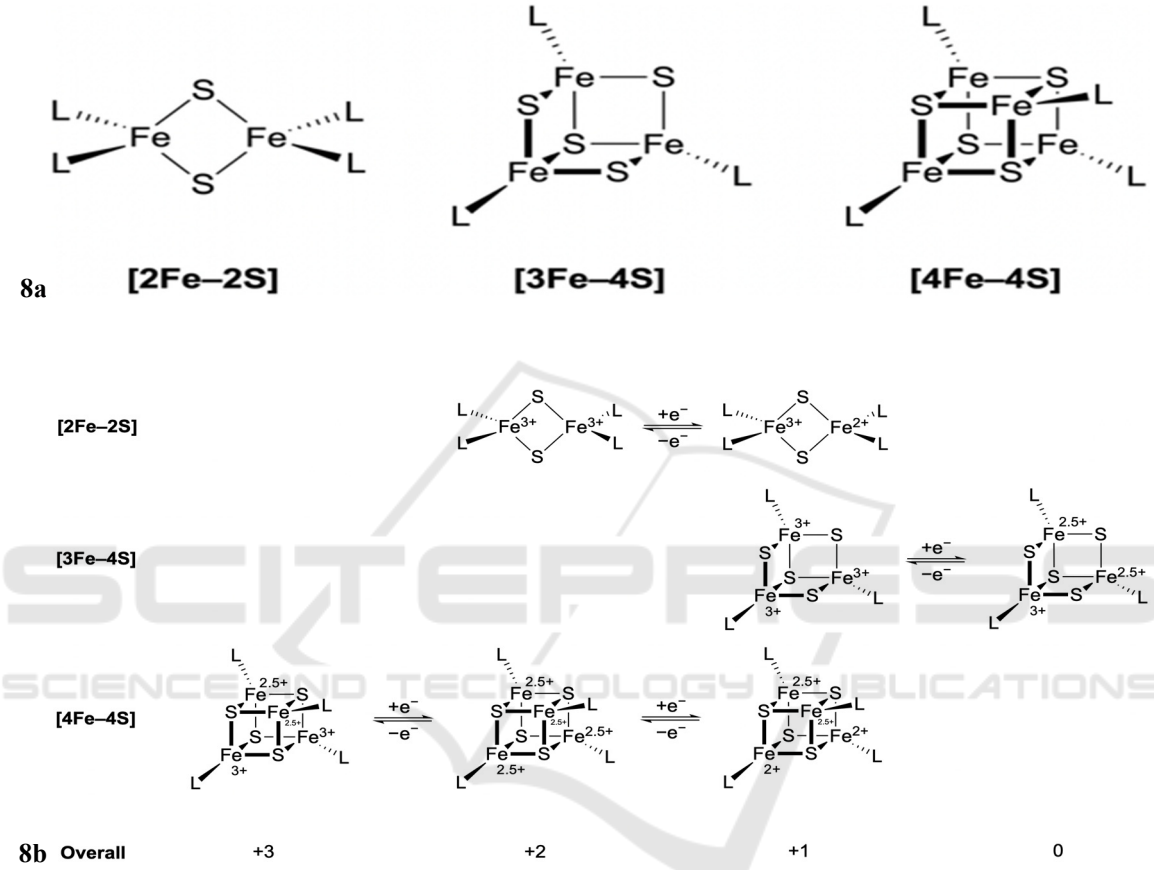

Figure 8: (a) Three common types of iron–sulfur clusters. L represents any ligand, often cysteine. Though [4Fe–4S] is cubic, it is not a perfect cube. This is similar for [3Fe–4S]. (b) Electron transfer mechanisms in the three common iron–sulfur clusters. The oxidation state of +2.5 is due to delocalized electrons, so they occur in pairs.

In prokaryotic nitrate reductases, all of the three common types of iron–sulfur clusters are present or possibly present. In NapA, there is a [4Fe–4S] near the active site (Figures 1 & 9b), which is the same for NarG. In NarH, the electron transfer subunit, there are three more [4Fe–4S] and one [3Fe–4S], which is at the side nearer to NarI, where two heme B are located (Figure 9a). On the contrary, the understanding of Nas is still limited and no crystal structures of Nas have been determined, so it can only be speculated based on genetic information that there may be a [4Fe–4S] near Mo-bis-MGD and additional [2Fe–2S] clusters (Richardson, 2007).

4.3 Hemes

Hemes are primarily composed of porphyrin rings, with an iron ion chelated by four nitrogen atoms from porphyrin's pyrrole rings. Based on different side chains, hemes are classified into different types, and the most common ones include heme B and heme C. Heme B is the precursor of other heme types and it is not attached to the protein, while heme C is anchored to the peptide chains through covalent bonding to thiolate groups of cysteines (Kim, 2018) (Figures 10 & 9c). The iron center of heme is often axially coordinated by histidine residues (Figure 9c),

because the protonation state of histidine can tune the redox potential, spin state and reactivity of the Fe ion (Bowman, 2008). Since the Fe ion has two oxidation states, +2 and +3, hemes can also facilitate electron transfer.

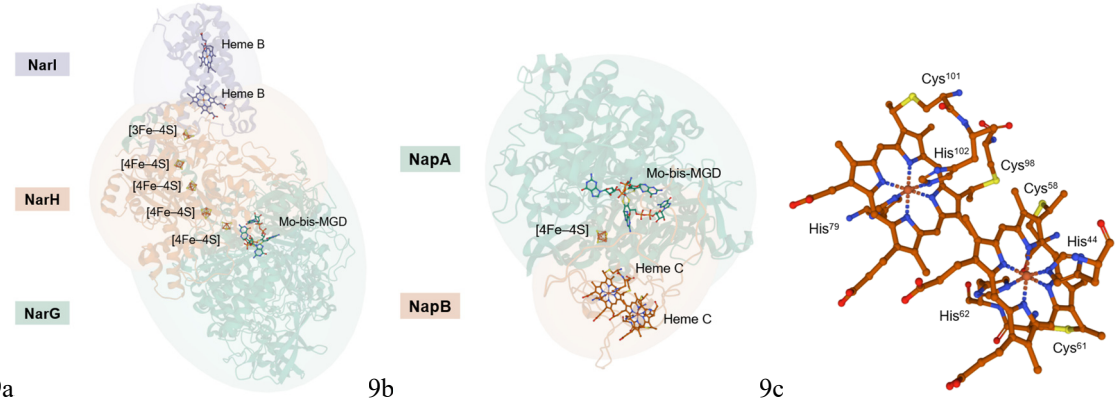

9a 9b 9c

Figure 9: (a) The overall structure of NarGHI of *E. coli* (PDB: 1Q16). All ligands binding to the labelled cofactors are hided. (b) The overall structure of NapAB of *Rhodobacter sphaeroides* (PDB: 1OGY). Ligands binding to heme C are not hided. (c) A zoom-in view of ligands at heme C. Each heme has two axial histidine ligands.

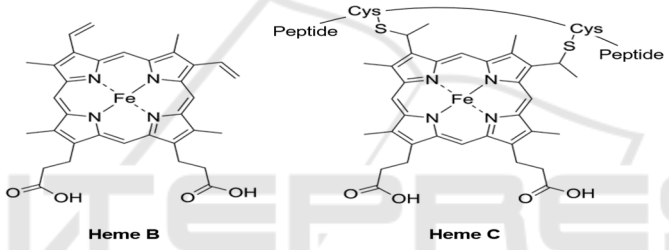

Figure 10: Structures of heme B and heme C.

Hemes are only present in Nar and Nap, as two different types. Two heme B are present in NarI and two heme C are present in NapB. Though crystal structures of NapC has not been determined, it also contains heme C. Hemes in NapB only act as electron carriers, but those in NapC and NarI have another function, which is to oxidize quinols (including ubiquinols and menaquinols) to their respective quinone form, hence generating two electrons necessary for NO_3^- reduction (Gates, 2011). For Nar, this process also releases two protons into the periplasm, hence creating a proton gradient for ATP synthesis (Figures 11 & 2). Although the possible quinol binding sites have been suggested (Bertero, 2005), there are no studies on the mechanism of quinol oxidation by NapC and NarI.

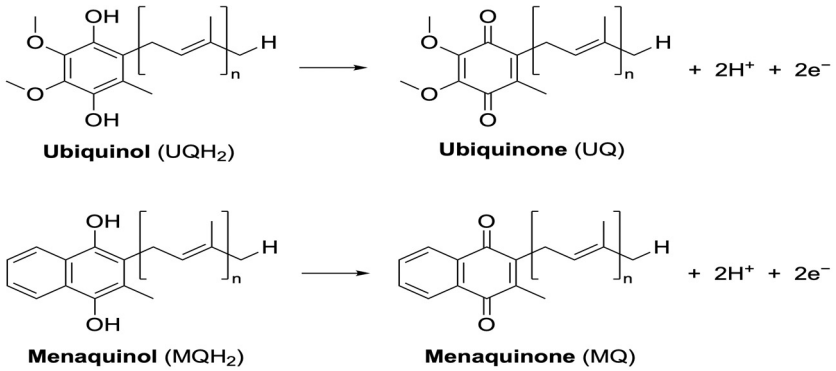

Figure 11: Chemical equation for oxidation of ubiquinols and menaquinols.

5 ELECTRON TRANSFER IN NITRATE REDUCTASES

5.1 Membrane-bound Respiratory Nitrate Reductase (Nar)

To form a complete redox loop and convert quinones back to quinols, another enzyme is required: formate dehydrogenase N (Fdn). It is structurally highly similar to Nar, with three subunits GHI, where FdnG contains a Mo-bis-MGD and a [4Fe–4S] cluster as NarG, FdnH contains four slightly different iron–sulfur clusters compared to NarH, and FdnI anchors the enzyme on plasma membrane as NarI, and contains two heme B and Q sites where quinones are reduced back to quinols (Figure 9a & 12a & 12b). NarGHI often forms dimers while FdnGHI forms trimers, and their orientations are different: the FdnG active site is inside the periplasm (Bertero, 2011) (Figure 12b).

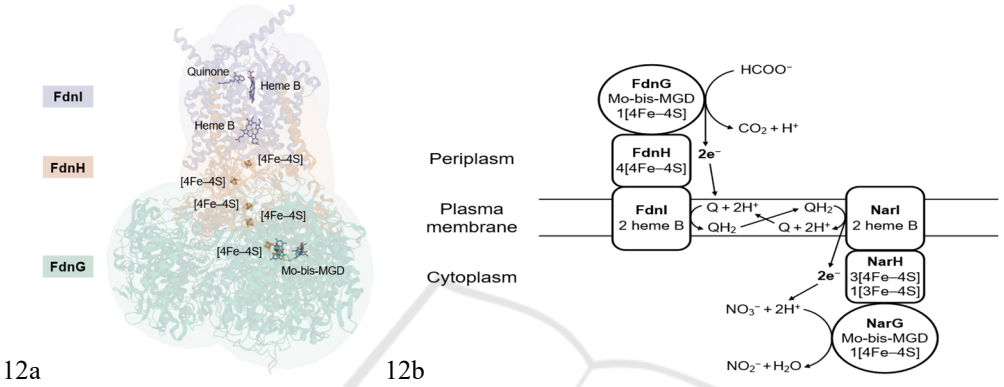

12a 12b

Figure 12: (a) Crystal structure of *E. coli* FdnGHI (PDB: 1KQG). The structure shows a trimer, but the cofactors of only one protein unit are shown. It also shows a quinone molecule at heme B, which is probably the substrate that is going to be reduced. (b) Simplified representation of the positions of FdnGHI and NarGHI relative to the plasma membrane. Electron transfers and the Q cycle are also shown.

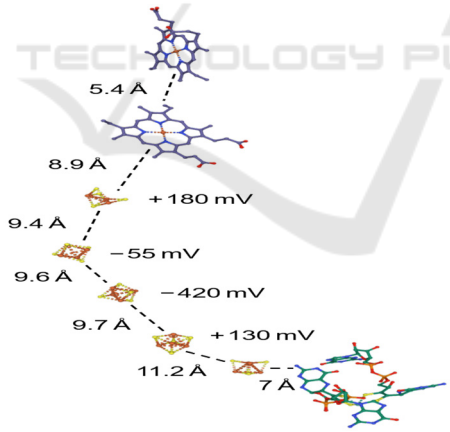

Figure 13: Distances between each electron transfer cofactor and respective redox potential values for iron–sulfur clusters in NarH. The values are for *E. coli* Nar, PDB: 1Q16.

The function of the FdnG active site is to oxidize formates ($HCOO^-$) to carbon dioxide (CO_2) and a proton, releasing two electrons which are then transferred through the [4Fe–4S] clusters in the electron transfer subunit FdnH to FdnI, where the Q site is located. Quinones accept the two electrons and are reduced to quinols, which are then used as the electron donor for NO_3^- reduction. In theory, this process releases two protons into the periplasm, but it seems that protons produced would be consumed by quinone reduction at FdnI, and thus conserved in the Q cycle. Despite this, there is still a net proton movement from the cytoplasm towards periplasm, because one proton is produced by the oxidation of formates while two are consumed in the oxidation of NO_3^-.

Some specific aspects of the route of electron transfer in Nar are also intriguing. The electron transfer cofactors are neatly aligned to form a structure functioning like an electrical wire (Figure 9a), where the distance between adjacent cofactors are all less than 14 Å, the distance limit for physiological electron transfer (Bertero, 2011) (Figure 13). However, the redox potential values determined in several *E. coli* Nar iron–sulfur clusters (Blasco, 2001) are not consistently arranged in a thermodynamically favorable order, with several large potential barriers (Figure 13). The reason is still unclear, but it may involve electron tunnelling (Page, 1999).

5.2 Periplasmic Nitrate Reductase (Nap)

Instead of iron–sulfur clusters, NapB uses two heme C molecules to facilitate electron transfer (Figure 9b). It also has a quinol-oxidizing subunit NapC with two heme C, whose crystal structure is yet to be determined. NapC is also anchored to the membrane (Figure 2).

Unlike Nar, it is believed that amino acid residues also play a part in the electron transfer pathway in Nap. In NapA, the distance between the Mo ion and the adjacent [4Fe–4S] cluster is about 12 Å, fairly close to the 14 Å limit, so a lysine residue which is hydrogen-bonded to the $-NH_2$ group of one of the MGD provides an electron transfer pathway (Sparacino-Watkins, 2014) (Figure 14). However, the mechanism is not stated.

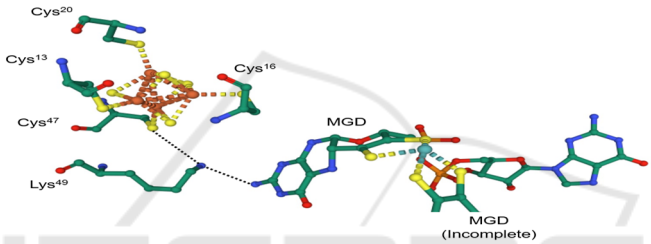

Figure 14: The lysine residue (Lys^{49}) which facilitates electron transfer in Nap of *E. coli* (PDB: 2NAP).

5.3 Prokaryotic Assimilatory Nitrate Reductase (Nas)

Since the major function of Nas is very different from that of Nar and Nap, its structure also deviates a lot from Nar and Nap. However, the current understanding on Nas is rather limited, and no crystal structures of any subunit of Nas have been determined.

Nas are free proteins located in the cytoplasm. They do not use the Q cycle as the electron source to reduce NO_3^-, so they do not contain hemes. Instead, Nas rely on flavodoxin or NADH as the electron source. Flavodoxin-dependent Nas gains electrons through the electron carrier flavin mononucleotide (reduced form, $FMNH_2$) via the oxidation $FMNH_2 \rightarrow FMN + 2H^+ + 2e^-$ and it is composed of a single subunit, while NADH-dependent Nas has one FAD-containing subunit receiving electrons from the oxidation of NADH through $NADH \rightarrow NAD^+ + H^+ + 2e^-$, and another catalytic subunit containing Mo-bis-MGD. Iron–sulfur clusters [4Fe–4S], [3Fe–4S] and [2Fe–2S] are probably all present for electron transfer, according to genetic information (Moreno-Vivián, 1999).

6 CONCLUSIONS

In conclusion, prokaryotic nitrate reductases all use a Mo-bis-MGD cofactor at the active site to catalyze nitrate reduction and iron–sulfur clusters to transfer electrons. Nar and Nap use the Q cycle as the electron source, so they both contain hemes, while Nas gains electron through flavodoxin or NADH, where heme is not required.

There are still lots of problems to solve in the field of nitrate reductases. The most completely studied nitrate reductase is Nar, because the crystal structure of NarGHI is clear, and data about redox potentials and distances between cofactors have all been determined. On the contrary, there is little structural information about Nas, where most are only speculations. There are also other intriguing aspects for future studies, such as the potential barrier inside NarH, the mechanism of quinol oxidation, and why Mo is the unique element involved in nitrate reduction.

REFERENCES

Bebout, G. E., Fogel, L. M., & Cartigny, P. (2013). Nitrogen: Highly Volatile yet Surprisingly Compatible. Elements, 9(5), 333-338.

Butler, C. S., Charnock, J. M., Bennett, B., Sears, H. J., Reilly, A. J., Ferguson, S. J., Garner, C. D., Lowe, D. J., Thomson, A. J., Berks, B. C., Richardson, D. J. (1999). Models for Molybdenum Coordination during the Catalytic Cycle of Periplasmic Nitrate Reductase from Paracoccus denitrificans Derived from EPR and EXAFS Spectroscopy. Biochemistry, 38(28), 9000-9012.

Broderick, J. B. (2004). Iron–Sulfur Clusters in Enzyme Catalysis. In J. A. McCleverty, & T. J. Meyer, Comprehensive Coordination Chemistry II: Bio-coordination Chemistry (Vol. VIII). Elsevier.

Brzóska, K., Męczyńska, S., & Kruszewski, M. (2006). Iron-sulfur cluster proteins: electron transfer and beyond. Acta Biochimica Polonica, 53(4), 685-691.

Beinert, H. (2000). Iron-sulfur proteins: ancient structures, still full of surprises. JBIC Journal of Biological Inorganic Chemistry, 5(1), 2-15.

Bowman, S. E., & Bren, K. L. (2008). The chemistry and biochemistry of heme c: functional bases for covalent attachment. Natural Product Reports, 25(6), 1118-1130.

Bertero, M. G., Rothery, R. A., Boroumand, N., Palak, M., Blasco, F., Ginet, N., Weiner, J. H., Strynadka, N. C. (2005). Structural and Biochemical Characterization of a Quinol Binding Site of Escherichia coli Nitrate Reductase A. Journal of Biological Chemistry, 280(15), 14836-14843.

Bertero, M. (2011). The membrane-bound nitrate reductase A from Escherichia coli: NarGHI. Encyclopedia of Inorganic and Bioinorganic Chemistry, 1-10.

Blasco, F., Guigliarelli, B., Magalon, A., Asso, M., Giordano, G., & Rothery, R. A. (2001). The coordination and function of the redox centres of the membrane-bound nitrate reductases. Cellular and Molecular Life Sciences, 58(2), 179-193.

Cabello, P., Roldán, M. D., Castillo, F., & Moreno-Vivián, C. (2009). Nitrogen Cycle. Encyclopedia of Microbiology, 299-321.

Cerqueira, N. M., Fernandes, P. A., Gonzalez, P. J., Moura, J. J., & Ramos, M. J. (2013). The Sulfur Shift: An Activation Mechanism for Periplasmic Nitrate Reductase and Formate Dehydrogenase. Inorganic Chemistry, 52(19), 10766-10772.

Dias, J. M., Than, M. E., Humm, A., Huber, R., Bourenkov, G. P., Bartunik, H. D., Bursakov, S., Calvete, J., Caldeira, J., Carneiro, C., Moura, J. J., Moura, I., Romão, M. J. (1999). Crystal structure of the first dissimilatory nitrate reductase at 1.9 Å solved by MAD methods. Structure, 7(1), 65-79.

Gates, A. J., Kemp, G. L., To, C., Mann, J., Marritt, S. J., Mayes, A. G., Richardson, D. J., Butt, J. N. (2011). The relationship between redox enzyme activity and electrochemical potential—cellular and mechanistic implications from protein film electrochemistry. Physical Chemistry Chemical Physics, 13(17), 7720-7731.

Jormakka, M., Richardson, D., Byrne, B., & Iwata, S. (2004). Architecture of NarGH Reveals a Structural Classification of Mo-bisMGD Enzymes. Structure, 12(1), 95-104.

Kuypers, M. M., Marchant, H. K., & Kartal, B. (2018). The microbial nitrogen-cycling network. Nature Reviews Microbiology, 16(5), 263-276.

Kim, H. J. (2018). Haem Structure and Function. eLS, 1-9.

Lippard, S. J., & Berg, J. M. (1994). Principles of Coordination Chemistry Related to Bioinorganic Research. In S. J. Lippard, & J. M. Berg, Principles of Bioinorganic Chemistry. University Science Books.

Moreno-Vivián, C., Cabello, P., Martinez-Luque, M., Blasco, R., & Castillo, F. (1999). Prokaryotic Nitrate Reduction: Molecular Properties and Functional Distinction among Bacterial Nitrate Reductases. Journal of Bacteriology, 181(21), 6573-6584.

Moura, J. J., Brondino, C. D., Trincão, J., & Maria João, R. (2004). Mo and W bis-MGD enzymes: nitrate reductases and formate dehydrogenases. JBIC Journal of Biological Inorganic Cheistry, 9(7), 791-799.

Page, C. C., Moser, C. C., Chen, X., & Dutton, P. (1999). Natural engineering principles of electron tunnelling in biological oxidation–reduction. Nature, 402(6757), 47-52.

Richardson, D. J., van Spanning, R. J., & Ferguson, S. J. (2007). The Prokaryotic Nitrate Reductases. In H. Bothe, S. Ferguson, & W. E. Newton, Biology of the Nitrogen Cycle. Elsevier.

Sparacino-Watkins, C., Stolz, J. F., & Basu, P. (2014). Nitrate and periplasmic nitrate reductases. Chem. Soc. Rev., 43(2), 676-706.

Stewart, L. J., Bailey, S., Bennett, B., Charnock, J. M., Garner, C. D., & McAlpine, A. S. (2000). Dimethylsulfoxide reductase: an enzyme capable of catalysis with either molybdenum or tungsten at the active site. Journal of Molecular Biology, 299(3), 593-600.